Supporting Information

Templated Construction of a Zn-Selective Protein Dimerization Motif

Eric N. Salgado, Jeffrey D. Brodin, Magnus M. To and F. Akif Tezcan*
Department of Chemistry and Biochemistry
University of California, San Diego
9500 Gilman Drive, MC 0356, La Jolla
CA 92093, U.S.A.
tezcan@ucsd.edu

The Supporting Information contains:
- Materials and Methods (pages S2-S3)
- Figures S1-S7 (pages S4-S9)
- Tables S1-S4 (pages S10-S12)
- Supporting References (page S13)

\

Materials and Methods

Protein Mutagenesis. Purification, Modification with Crosslinkers

The G82C-RIDC1 cyt cb_{562} construct was generated, expressed, and purified according to published procedures [1]. Purified ^{C82}RIDC1 was buffer exchanged into 20 mM TRIS (pH 7) and 50 mM dithiothreitol (DTT) and concentrated using Amicon stirred cells with MW=10 kDa cutoff-filters. Concentrated protein was eluted through a 10 DG desalting column (BioRad) to eliminate excess DTT) and diluted with an appropriate volume of 20 mM TRIS (pH 7) to yield a protein concentration of 100 μM. Concentrated stock solutions of BMOE, BMB, or BMH (Pierce) were added to the sample in ten equal aliquots every 30 sec over 5 min to give a final crosslinker concentration of 100 μM. The reaction was then allowed to proceed at room temparature under constant stirring for 30 min. Crosslinking reactions were quenched by the addition of 50 mM DTT and allowed to incubate at room temperature for 15 min. Crosslinking yields were ca. 50%. Crosslinked proteins were subsequently purified through multiple size exclusion chromatography runs using a Pall ACA54 resin (fractionation range = 5-70 kDa) using an elution buffer of 20 mM TRIS (pH 7) and 150 mM NaCl until all monomeric protein was separated out. Dimer purity was assessed by SDS-PAGE electrophoresis and the compositions of the dimers were verified by MALDI mass spectrometry.

Analytical Ultracentrifugation and SV simulations

Sedimentation velocity (SV) measurements were made on a Beckman XL-I Analytical Ultracentrifuge (Beckman-Coulter Instruments) using an An-60 Ti rotor at 41,000 rpm for a total of 250 scans per sample. Data were collected at 415 nm for low concentration (2.5 μM crosslinked dimer, 5 μM RIDC1 monomer) samples, and 560 nm for higher concentrations (25 μM crosslinked dimer). All data were processed in SEDFIT[2] with the following fixed parameters: buffer density (r) = 0.99764 g/ml; buffer viscosity = 0.0089485 poise; Vbar, which was calculated to be 0.7310 ml/g for ^{BMOE}RIDC1$_2$ and ^{BMB}RIDC1$_2$; 0.7306 ml/g for ^{BMH}RIDC1$_2$. The buffer density (ρ) and viscosity for 20 mM TRIS (pH 7) were calculated through SEDNTERP (http://www.jphilo.mailway.com/default.htm). Theoretical sedimentation coefficients were calculated using Hydropro Version 7.C,[3] using the same parameters employed in SV data processing.

Crystallography

The crystals for all crosslinked dimers were obtained by sitting drop vapor diffusion at room temperature. The crystallization conditions for the four different crystal forms described in this study, as well as the corresponding data collection and refinement statistics, are listed in Table S1 and Table S2, along with data collection and refinement statistics. All protein stocks solutions were in 20 mM TRIS (pH 7) buffer. Appropriate crystals were transferred to a solution of mother liquor containing 20% glycerol as cryoprotectant and frozen in liquid nitrogen prior to data collection at 100 K.

Data were integrated using MOSFLM and scaled in SCALA,[4] except for Zn_4:^{BMB}RIDC1$_4$, which was processed using SAINT and Bruker SADABS. All structures were determined through molecular replacement with MOLREP,[5] using the RIDC1 monomer structure (PDB ID:3HNI) as the search model, followed by rigid-body, positional, thermal and TLS refinement with REFMAC[6] using appropriate non-crystallographic symmetry restraints. The crystals for both forms of Zn_4: ^{BMOE}RIDC1$_4$ (crystallized in the presence and the absence of

$CuSO_4$) were found to have 48% and 44% twin fractions, respectively. Both data sets were refined using intensity based twin refinement as implemented in REFMAC using the twin operator: -1.000H-1.000K, 1.000K, -L. All models were manually rebuilt in COOT[7] to produce the final models. All figures were produced using PYMOL.[8]

Metal Binding Titrations

For Mag-Fura-2 competition titrations, 1 mg Mag-Fura-2 (Invitrogen) was resuspended in 1 ml Millipore purified water. Mag-Fura-2 concentration was determined using an extinction coefficient of 22,000 $M^{-1}cm^{-1}$ at 369 nm. The titrations for determining Mag-Fura-2 affinities for Ni^{II} and Co^{II} were performed in a 1-cm cuvette with a 2 ml sample volume containing 0.5 μM Mag-Fura-2 and 1 mM $CaCl_2$ in Chelex-treated 20 mM 3-(N-morpholino)propanesulfonic acid (MOPS, pH 7) buffer with 150 mM NaCl. The sample was allowed to equilibrate with stirring for 3 min. after each addition of the competing metal stock before recording fluorescence excitation scans monitoring emission at 505 nm. Zn^{II} titrations were performed with 1 mM Ni^{II} (sulfate salt) as the competing ion in place of $CaCl_2$. Titration data (fluorescence excitation monitored at 330 nm) were fit to a 1-site binding model using Dynafit[9] assuming a Mag-Fura-2:Ca^{2+} K_d of 25 μM, which was found to be constant over a wide variety of pH and ionic strength conditions.[10] The resulting K_d values are listed in Table S4. The Mag-Fura-2:Zn^{II} K_d was backed out using the Mag-Fura-2:Ni^{II} K_d determined here.

$^{BMOE}RIDC1_2$/Mag-Fura-2 competition assays were performed in a 1-cm cuvette with a 1.5-ml sample volume containing 25 μM $^{BMOE}RIDC1_2$ and 10 μM Mag-Fura-2 in Chelex-treated MOPS (pH 7) buffer with 150 mM NaCl. As with the titrations described above, samples were allowed to equilibrate under stirring for 3 min. after the addition of each aliquot of the appropriate divalent metal stock before recording fluorescence excitation scans monitoring emission at 505 nm. Ni^{II} and Co^{II} binding to Mag-Fura-2 results in quenching of the florescence signal, which was subsequently followed using the emission readout using 372 nm excitation. Zn^{II} binding results in an increased fluorescence excitation at 323 nm, which was used as the excitation wavelength. All titration curves could be adequately described with a minimal (4 × 1) binding model consisting of four binding sites with equivalent half-saturation values listed in Table S4. Cu^{II} titrations were performed similarly to Ni^{II}, Co^{II} and Zn^{II}, except Mag-Fura-2:Cu^{II} binding was monitored by absorbance increases at 300 nm, rather than by fluorescence.

Analytical Size Exclusion Chromatography (SEC)

Size exclusion chromatography was performed on a Biologic DuoFlow FPLC system (Bio-Rad) equipped with a UV detector set to monitor absorbance at 280 nm. For each run, 100 μl of 25 μM $^{BMOE}RIDC1_2$ in 20 mM TRIS (pH 7) buffer with 50mM NaCl and either 50 μM $ZnCl_2$ or 5 mM EDTA were injected on an analytical SEC column (GE Healthcare) packed with Pall ACA54 resin (fractionation range = 5-70 kDa). The samples were eluted from the column at 0.5 ml/min in 20 mM TRIS (pH 7) with 50 mM NaCl, and additionally, 5 mM EDTA for the metal free sample. The dead volume in Fig. S7 is based on a ferritin (MW ~ 500 kDa) standard run under conditions identical to the metal free sample.

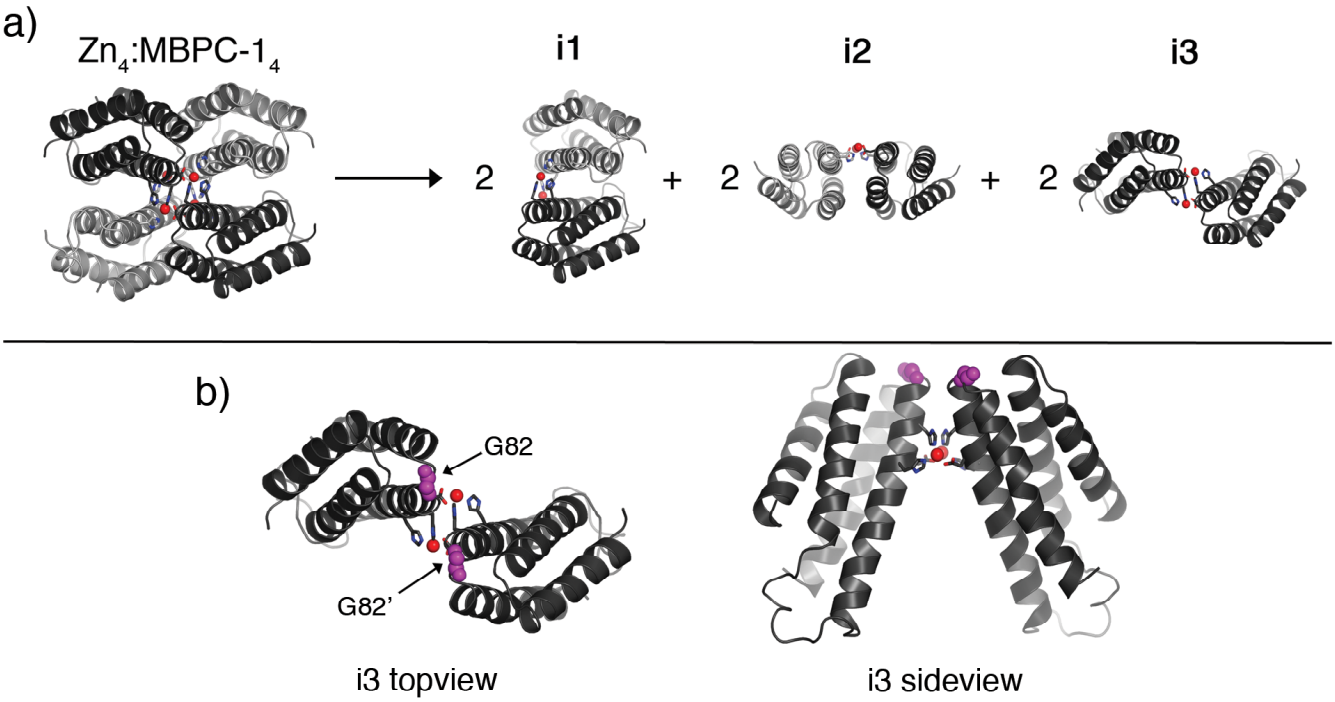

Figure S1. Detailed view of the three orthogonal C_2-symmetrical interfaces of Zn_4:MBPC1$_4$. a) Top views of interfaces *i*1, *i*2 and *i*3. b) Close-up top and side views of *i*3, highlighting metal coordination and position 82 used for crosslinking.

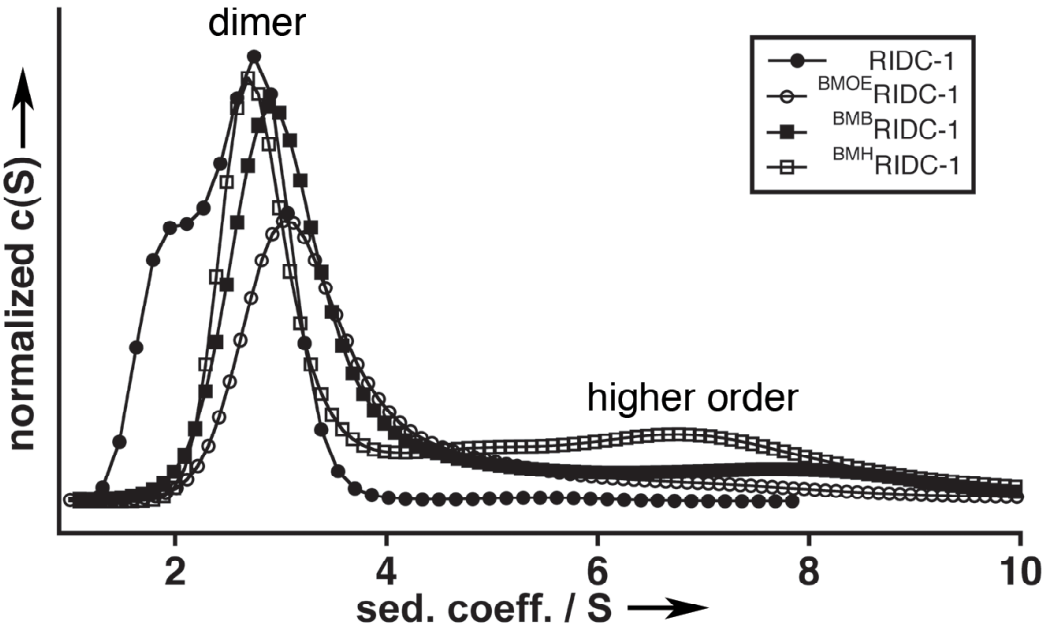

Figure S2. Sedimentation velocity profiles of 25 μM RIDC-1 or 25 μM crosslinked dimers in the presence of 5 mM EDTA, showing the presence of higher order aggregates for the latter species in addition to dimers.

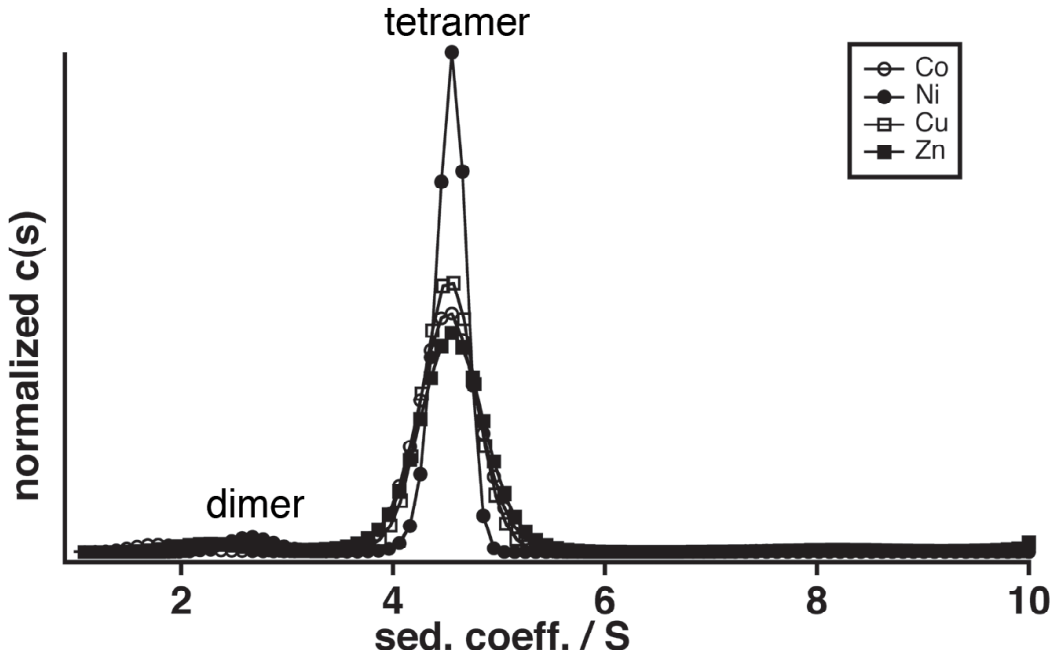

Figure S3. Sedimentation velocity profiles of 2.5 μM ^{BMOE}RIDC1$_2$ in the presence of 5 μM Co^{II}, Ni^{II}, Cu^{II} and Zn^{II}.

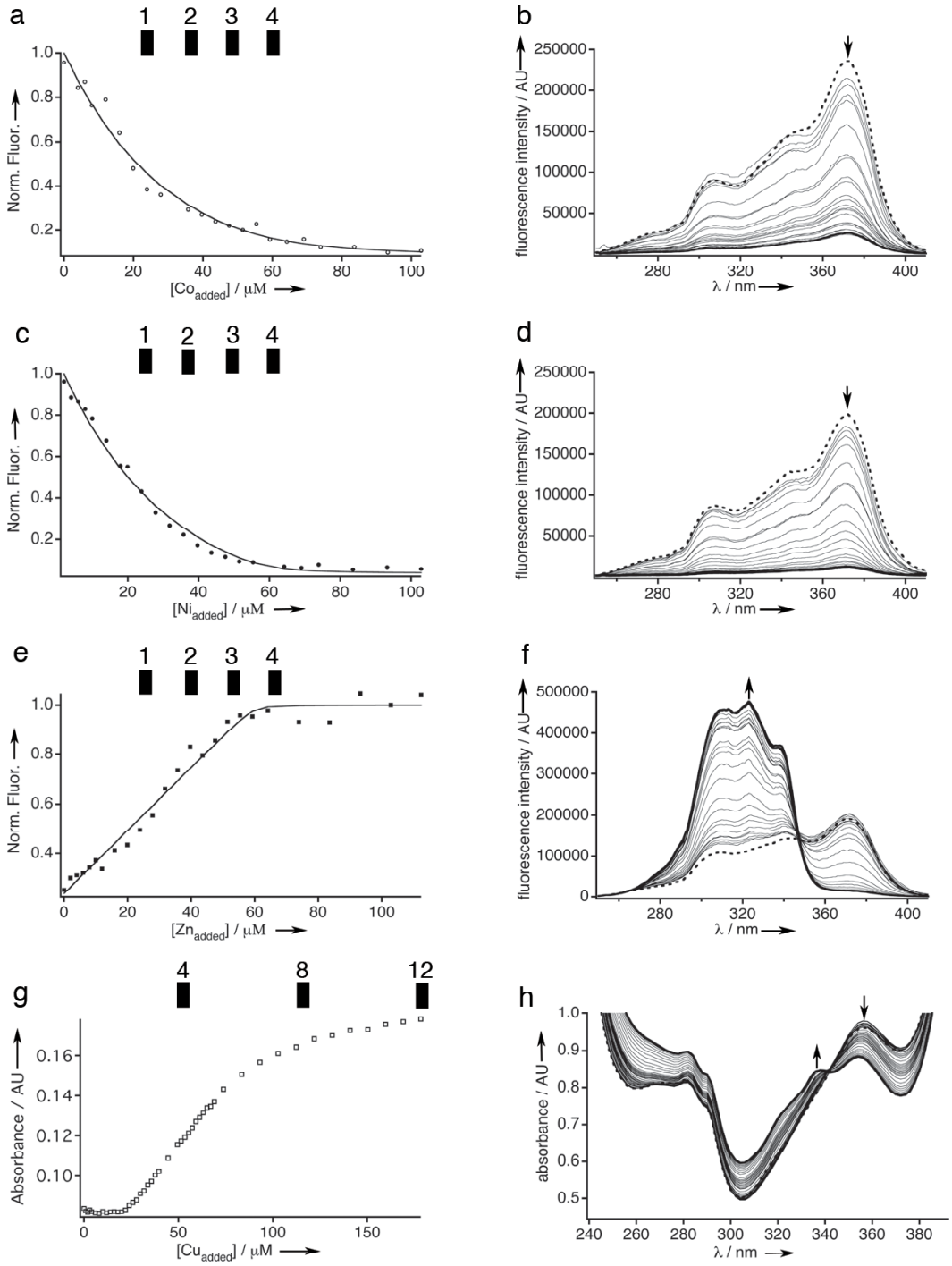

Figure S4. (a) Co^{2+}, (c) Ni^{2+}, and (e) Zn^{2+} binding isotherms for Mag-Fura-2 / $^{BMOE}RIDC1_2$ competition experiments and corresponding fluorescence excitation scans (b), (d) and (f). The tick marks shown on the top x-axis correspond to theoretical titration end points for the indicated number of binding sites per tetramer. Solid lines represent fits obtained using DynaFit to a four-equivalent-binding-sites model, with K_d values listed in Table S3. Cu^{2+} competition experiments (g, h) demonstrate the 12 metal binding events.

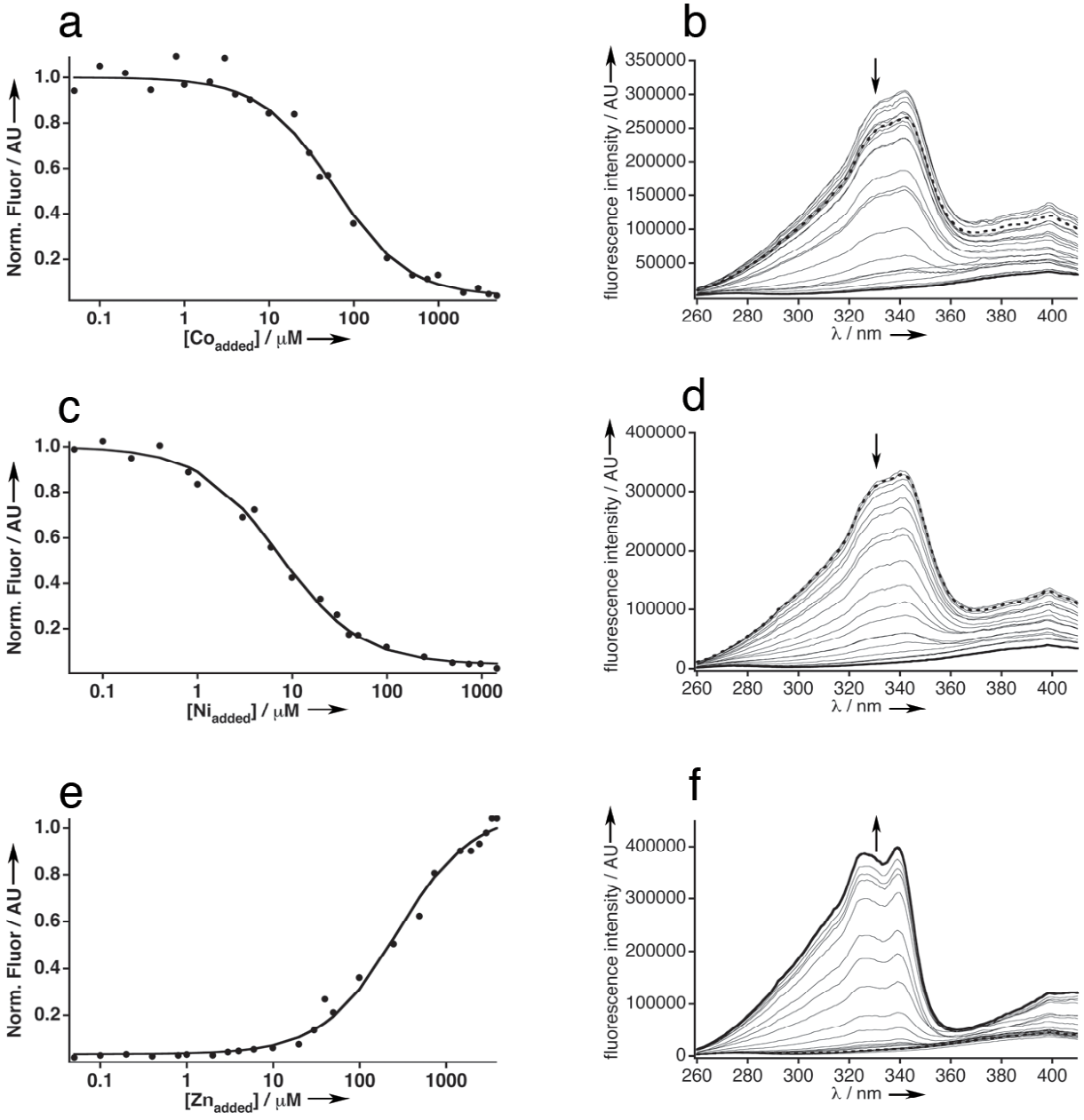

Figure S5. (a) Co^{2+}, (c) Ni^{2+}, and (e) Zn^{2+} binding isotherms for the determination of the divalent metal binding affinities of Mag-Fura2 and corresponding fluorescence excitation scans (b), (d) and (f). Solid lines represent fits obtained using DynaFit to a one-binding-site model. K_d's obtained from these fits are listed in Table S3.

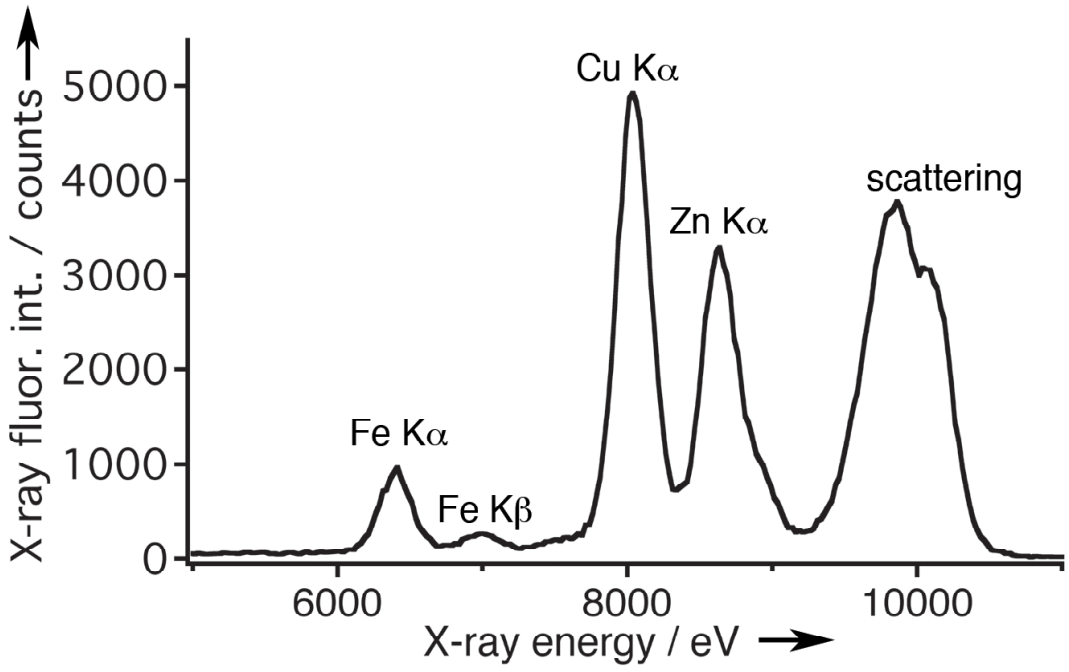

Figure S6. X-ray fluorescence scan (excitation at the Zn K-edge) of a single crystal of Zn_4:^{BMOE}RIDC1$_4$ cocrystallized with Cu^{II}, showing the presence of Fe (heme), Cu and Zn ions. The crystal was thoroughly washed with metal-free cryoprotectant solution to eliminate excess metal not incorporated into the crystal lattice.

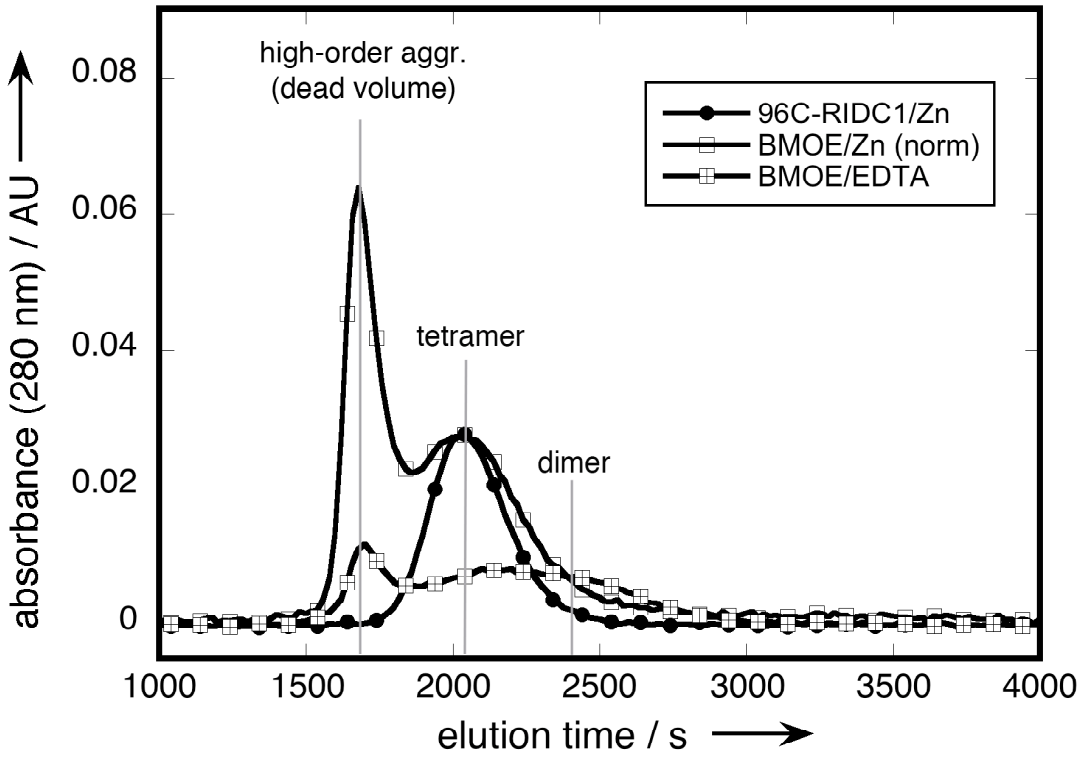

Figure S7. Size exclusion chromatograms of $^{C96}RIDC1_4$ in the presence of Zn and $^{BMOE}RIDC1_2$ (preloaded with Zn) in the presence of Zn^{II} or EDTA. $^{C96}RIDC1_4$ elutes as a single peak, indicative of a tetrameric species, whereas the $^{BMOE}RIDC1_2$ sample run in the presence of Zn^{II} contains a high molecular weight species that elutes in the void volume (measured using ferritin as a standard) and a second peak that is broadened towards the dimeric species relative to $^{C96}RIDC1_4$. This indicates that Zn_4:$^{BMOE}RIDC1_4$ can dissociate into a dimeric form in solution. For ease of comparison, the height of the BMOE/Zn tetramer peak (ca 2000 s.) was normalized to that of $^{C96}RIDC1$.

	Zn_4:^{BMOE}RIDC-1_4	Zn_4:^{BMOE}RIDC-1_4 / Cu
Mother liquor	100 mM HEPES pH 7.5, 10% PEG 3350, 4.6 mM $ZnCl_2$	100 mM HEPES pH 7.5, 12% PEG 3350, 2.46 mM $CuSO_4$
Concentration of protein	1.15 mM	2.46 mM
µl protein : µl mother liquor	2:1	1:1
X-ray source	SSRL BL 9-2	SSRL BL 7-1
Residues in complex	4 x (106 + 1 Heme) + 4 Zn	4 x (106 + 1 Heme) + 4 Zn
No. of complexes / asymmetric unit	1	1
Metal ions in asymmetric unit	13 Zn	6 Zn, 8 Cu
Waters in asymmetric unit	23	12
Unit cell dimensions (Å)	a = b =52.088, c = 253.943	a = b = 52.525, c = 255.717
	$\alpha = \beta = 90^\circ, \gamma = 120^\circ$	$\alpha = \beta = 90^\circ, \gamma = 120^\circ$
Symmetry group	$P6_1$	$P6_1$
Resolution (Å)	42.51 - 2.30	42.86 - 2.64
X-ray wavelength (Å)	0.9795	1.265 (near Zn K edge) 1.377 (Cu K edge)
Number of Unique Reflections	15859	10404
Redundancy	11.1	15.8
Completeness (%)*	99.3 (99.1)	97.9 (97.0)
(I / σI)*	10.6 (3.1)	3.8 (1.8)
R_{sym} (%)*	5.2 (24.8)	12.0 (36.2)
R_{cryst} (%)*	24.2 (31.9)	26.1 (33.6)
R_{free} (%)*	28.6 (46.0)	30.6 (40.3)
Rms Bnd (Å)	0.025	0.022
Rms Ang (°)	1.805	1.730
Ramachandran plot (%)		
Residues in most favored regions	94.4	94.1
Residues in add.l allowed regions	5.6	5.6
Residues in generously allowed regio	0.0	0.3
Residues in disallowed regions	0.0	0.0

Table S1. Crystallization conditions and data collection/refinement statistics for Zn_4:^{BMOE}RIDC1_4 and Zn_4:^{BMOE}RIDC1_4 cocrsytallized with Cu^{II}. * denotes highest resolution shell.

	Zn_4:^{BMB}RIDC-1_4	Zn_4:^{BMH}RIDC-1_4
Mother liquor	100 mM Bis-TRIS pH 6.5, 14% PEG 3350, 2.84 mM $ZnCl_2$	50 mM Bis-TRIS pH 6.5, 20% pentaerythritol ethoxylate [15/4 EO/OH], 200 mM ammonium sulfate, 2.12 mM $ZnCl_2$
Concentration of protein	710 μM	1.07 mM
μl protein : μl mother liquor	2:1	1:1
X-ray source	Bruker Apex II CCD detector and monochromatized Cu-Kα radiation (Siemens sealed tube source)	SSRL BL 9-2
Residues in complex	4 x (106 + 1 Heme) + 4 Zn	4 x (106 + 1 Heme) + 4 Zn
No. of complexes / asymmetric unit	1	1
Metal ions in asymmetric unit	4	5
Waters in asymmetric unit	434	12
Unit cell dimensions (Å)	63.626 x 76.399 x 93.265	48.298 x 61.843 x 70.087
	$\alpha = \beta = \gamma = 90^\circ$	$\alpha = \gamma = 90^\circ$, $\beta = 102.22^\circ$
Symmetry group	$P2_12_12_1$	$P2_1$
Resolution (Å)	22.55 - 1.84	47.20 - 2.70
X-ray wavelength (Å)	1.542	0.9795
Number of Unique Reflections	37038	10569
Redundancy	4.6	3.7
Completeness (%)*	99.4 (97.9)	100.0 (100.0)
(I / σI)*	14.55 (3.19)	2.5 (6.5)
R_{sym} (%)*	5.7 (32.4)	9.3 (10.4)
R_{cryst} (%)*	19.0 (26.4)	28.8 (34.4)
R_{free} (%)*	24.3 (35.7)	31.8 (37.7)
Rms Bnd (Å)	0.024	0.015
Rms Ang (°)	1.96	1.56
Ramachandran plot (%)		
Residues in most favored regions	97.4	94.1
Residues in add.l allowed regions	2.6	5.9
Residues in generously allowed regior	0.0	0.0
Residues in disallowed regions	0.0	0.0

Table S2. Crystallization conditions and data collection/refinement statistics for Zn_4:^{BMB}RIDC1_4 and Zn_4:^{BMH}RIDC1_4. * denotes highest resolution shell.

Metal	K_d (μM)	
	Mag-Fura-2	^{BMOE}RIDC-1_2
Zn	0.047 (0.005)	0.041 (0.010)
Ni	0.175 (0.014)	0.54 (0.055)
Co	1.41 (0.22)	9.29 (1.02)

Table S3. K_D values for divalent metal ion adducts of Mag-Fura2 and ^{BMOE}RIDC-1_2.

[1] a)E. N. Salgado, J. Faraone-Mennella, F. A. Tezcan, *J. Am. Chem. Soc.* **2007**, *129*, 13374; b)E. N. Salgado, R. A. Lewis, J. Faraone-Mennella, F. A. Tezcan, *J. Am. Chem. Soc.* **2008**, *130*, 6082; c)E. N. Salgado, R. A. Lewis, S. Mossin, A. L. Rheingold, F. A. Tezcan, *Inorg. Chem.* **2009**, *48*, 2726.
[2] P. Schuck, *Biophys. Chem.* **2004**, *108*, 187.
[3] J. G. de la Torre, M. L. Huertas, B. Carrasco, *Biophys. J.* **2000**, *78*, 719.
[4] Collaborative Computational Project, Number 4. 1994. "The CCP4 Suite: Programs for Protein Crystallography". Acta Cryst. D50, 760-763
[5] A. Vagin, A. Teplyakov, *J. Appl. Cryst.* **1998**, *30*, 1022.
[6] G. Murshudov, A. Vagin, E. Dodson, *Acta Cryst.* **1996**, *D53*, 240.
[7] P. Emsley, K. Cowtan, *Acta Cryst.* **2004**, *D60*, 2126.
[8] W. L. DeLano, *The PYMOL Molecular Graphics System (http://www.pymol.org)*, **2003**.
[9] P. Kuzmic, *Anal. Biochem.* **1996**, *237*, 260.
[10] F. A. Lattanzio, D. K. Bartschat, *Biochem. Biophys. Res. Comm.* **1991**, *177*, 184.